

Investigating the Kinetics and Regioselectivity of a 1,3-dipolar Cycloaddition using NMR Spectroscopy, GC-MS, and *In Silico* Orbital Analysis

Alex Cumming

Abstract

Here we investigate the regioisomerism of a 1,3-dipolar cycloaddition and the effects of para-dipolarophile substituents on rate. Reaction products were analyzed using $^1\text{H-NMR}$ and GC-MS, and rate data was collected using a $^1\text{H-NMR}$ pulse program to collect multiple 1D spectra over time. Electrostatic and orbital energy data were also gathered *in silico* using Spartan software. We observed exclusive formation of 3,5-diphenyl isoxazoline products in accordance with computationally predicted electrostatics of participating atoms. Even though dipolarophiles with more electron-withdrawing groups had decreased orbital energy gaps to a consistent dipole, we observed a decrease in reaction rate for dipolarophiles with greater electron-withdrawing character. Our upside down V-shaped trend on the Hammett rate plot may indicate a changing mechanism for the cycloaddition between electron-donating and electron-withdrawing substituents.

Introduction

A well-known synthetic method of forming heterocycles is the 1,3-dipolar cycloaddition, also known as the Huisgen reaction after the chemist who first presented it.¹ In this type of reaction, a three-membered dipole contributes 4 π -system electrons and a two-membered dipolarophile contributes 2π electrons to combine to form a five-membered ring. One specific 1,3-dipolar cycloaddition involves the generation of a dipole from a readily available oxime in the presence of bleach.² Combined with readily available alkene dipolarophiles, a five-membered ring is formed.² With styrene, two regioisomers may be formed; Gingrich and Pickering² reported that these isomers can be distinguished by $^1\text{H-NMR}$ spectroscopy but did not detail the ratio in which they are formed. The kinetics of the reaction can

be studied at low concentrations in the presence of a liposome membrane.³ Svatoněk et al.⁴ and Dones et al.⁵ have more recently found ways to accelerate the rate of 1,3-dipolar additions through stabilization of the dipole by F⁻ ions⁴ and reactant-reactant hydrogen bonding.⁵

In our experiment, we investigated substituent effects on the rate of the 1,3-dipolar addition originally demonstrated by Gingrich and Pickering.² We sought to understand how various electron donating and withdrawing substituents affect the rates of these cycloadditions. After trying a variety of spectroscopic techniques, we settled on using pseudo-2D NMR spectroscopy as the most reliable method to gather concentration data for use in kinetics analysis. We also relied on NMR spectroscopy to verify product formation and explore the regioselectivity resulting in possible 3,4- and 3,5-diphenyl isomers.

Formation of a 3,5-diphenyl isomer was favored exclusively for both styrene and 4-chlorostyrene, and can be expected for other substituted styrenes due to electrostatic trends. Kinetic data was acquired by preserving the activated dipole in deuterated chloroform (CDCl_3) at concentrations used by Iwasaki et al.³ and taking multiple 1D NMR spectra over time. Increasing substituent σ value may increase reaction rate up to a point, then decrease it as substituents become more electron-withdrawing.

Experimental Methods

NMR

We collected NMR spectra using a Bruker 500 MHz spectrometer and TopSpin software. Data was processed via Fourier transform analysis. Samples were dissolved in CDCl_3 containing 0.03% TMS (Sigma-Aldrich).

Gas Chromatography–Mass Spectrometry (GC-MS)

Spectra were collected on an Agilent 890 GC-MS and were analyzed using Agilent Masshunter software.

GC Peaks were analyzed with Masshunter software.

Investigating Reaction Kinetics using GC-MS

Reactions for kinetic studies were run according to the procedure found in Gingrich and Pickering.² Anisole (25 μ L) was added to the reaction mixture as an internal standard for GC. Approximately 5 drops of the reaction mixture was removed from the test-tube every 6 minutes, and then extracted with ethyl acetate to remove any water from the sample. The test-tube was vortexed using a benchtop vortexer everytime a sample was removed from the test-tube to recombine the aqueous and organic layers prior to sample removal. The organic ethyl acetate layer (100 μ L) was diluted with CH_2Cl_2 (1 mL) in a GC-MS vial for further analysis.

Cycloaddition Reactions

We added 2.27 mmol of benzaldehyde oxime (BO) and three drops of triethylamine (TEA) to 1 mL of DCM to perform the dipole-dipolarophile additions according to Gingrich and Pickering.² We also prepared the BO and TEA in chloroform (CHCl_3) to explore whether the reaction could be run in a more readily available solvent for NMR spectroscopy. Then, we added an excess (8.73 mmol) of styrene, chlorostyrene, or acetoxystyrene to the reaction mix. To this solution we added 6 mL bleach (NaClO) in 2 mL aliquots with vortex mixing and cooling in between additions. After one hour of mixing every six minutes at room temperature, we rotovapped the reaction mix and left products one week to dry. We then recrystallized using Gingrich and Pickering's² recommendation for ethanol as a recrystallization solvent.

Reaction Product Quantifications

δ = chemical shift (ppm); s = singlet, m = multiplet, dd = doublet of doublets; #H indicates relative integration. t_r = retention time; m/z = mass-to-charge ratio for molecular ion; all GC-MS runs were performed using ethyl acetate (EtOAc) as solvent.

Product from styrene. $^1\text{H-NMR}$ δ 7.71 (s, 2H), 7.40 (m, 7H), 7.07 (s, 1H), 5.79 (dd, 1H), 3.83 (dd, 1H), 3.40 (dd, 1H). GC-MS (EtOAc): t_r 13.19 min, m/z 223. Expected m/z 223.
Product from chlorostyrene (crude). GC-MS (EtOAc): t_r 14.26 min, m/z 257. Expected m/z 257.
Product from acetoxystyrene (crude). GC-MS (EtOAc): t_r 15.30 min, m/z 281. Expected m/z 281.

Investigating Reaction Kinetics Using NMR

We scaled down the reaction volume from Gingrich and Pickering² by a factor of 16 (mmol scale) in order to run it in a 5 mm NMR tube for possible NMR application. The instrument failed to lock onto the sample, preventing further exploration. Extracting the active BO dipole and TEA into CDCl_3 (as performed by Iwasaki et al.³ into propanol) and adding this mixture into the NMR tube allowed us to successfully measure kinetics by running a $^1\text{H-NMR}$ pulse program (Td-30, D20-60sec, NS-4) and create a pseudo-2D NMR dataset.

Investigating Reaction Kinetics Using UV/Vis

We attempted to replicate the UV/Vis kinetics measurements performed by Iwasaki et al.³ with styrene instead of the authors' original maleimide. We performed the cycloaddition reaction in 1-propanol and reduced reagent concentrations to fit within the absorbance profile of the spectrophotometer. Failure to detect a change in λ_{max} or in absorbance at λ_{max} of our product (265 nm) prevented us from performing further experiments.

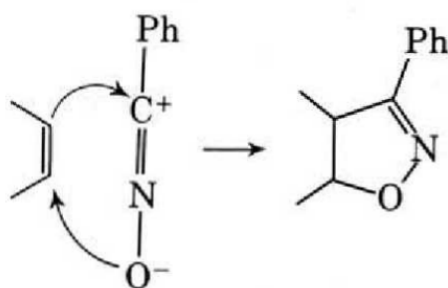
Computational Analysis

We used Spartan '20 software to calculate HOMO-LUMO gaps between the dipole and dipolarophile reactants. Calculations were performed using the Hartree-Fock method and the 6-31G* basis set.

Results and Discussion

Bulk Reaction and Product Analysis

We investigated the product and kinetics of the 1,3-dipolar addition described in Gingrich and Pickering² (Scheme 1). Their original reaction involved activating benzaldehyde oxime with bleach (NaClO) as the dipolar nucleophile and cis or trans stilbene and styrene as the dipolarophile. For styrene, two regioisomers may form, a 3,4-diphenyl or a 3,5-diphenyl isoxazoline (Figure 2). Our initial investigations focused on (1) identifying the regioisomers of the products and (2) determining whether the reaction, which was originally run in dichloromethane (DCM), could also be run in chloroform for potential kinetics applications using a more readily available $^1\text{H-NMR}$ solvent.



Scheme 1: 1,3-dipolar cycloaddition reaction from Gingrich and Pickering.² We modified the alkene dipolarophile of this 1,3-dipolar cycloaddition, investigating substituted styrenes rather than 2-butene (see Figure 2).

While running the reaction in bulk with styrene as the dipolarophile, we observed a light-green colored aqueous top layer and a cloudy organic bottom layer (Figure 1). This observation was the same whether the reaction was run in DCM (following Gingrich and Pickering's² procedure) or chloroform. When running the reaction with acetoxystyrene and 4-chlorostyrene, the solutions were beige and light-green, respectively (Figure 1). Though chloroform ($D=1.49 \text{ g/cm}^3$) and DCM ($D=1.33 \text{ g/cm}^3$) are both more dense than water, our original styrene product was likely residing in a colored organic top layer since in both cases the top layer's volume ($\sim 2\text{mL}$) was less than that of the aqueous layer ($\sim 6\text{mL}$). Our bulk reactions for chlorostyrene and acetoxystyrene were more ambiguous, forming colored suspensions. This difference in appearance was likely due to reagents and products containing the additional chloro/acetoxo groups being more soluble due to the additional polar bonds/regions. The end goal of these reactions was product isomer analysis, and in all cases we were able to isolate sufficient product for analysis.

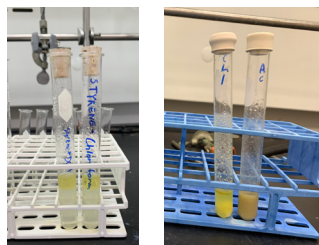


Figure 1: Images of (left to right) reactions of activated benzaldehyde oxime with styrene dipolarophile in DCM; styrene dipolarophile in chloroform; 4-chlorostyrene dipolarophile in DCM; and 4-acetoxystyrene in DCM. Despite differences in appearance, all reactions yielded sufficient product for NMR analysis and product confirmation.

Depending on the regioselectivity of the reaction, a 3,4-diphenyl or 3,5-diphenyl isomer may be observed (Figure 2). Gingrich and Pickering² did not specify which isomer is formed but suggested that product NMR would be useful for structure assignment. Following our bulk reactions, we purified our product formed with a styrene dipolarophile by recrystallization in ethanol.² Recrystallization yielded small white crystals from which we obtained an NMR spectrum (Figure 3). The predicted peaks for the 3,5-diphenyl product matched our spectrum more closely than the peaks for the 3,4-diphenyl isomer (Figure S1) indicating that the reaction had formed the 3,5-diphenyl structure. The hydrogen(s) adjacent to the oxygen of the ring will be the most downfield after the aromatic protons, and only one H is observed with our product at $\delta 5.79 \text{ ppm}$ (Figure 3). This methine proton experiences deshielding from the neighboring oxygen atom and the aromatic phenyl group. For the 3,4-diphenyl isomer, we would expect two H in this region with one upfield, but instead we observe that one H at $\delta 5.79 \text{ ppm}$ and two H in the at $\delta 3\text{-}4 \text{ ppm}$ region, pointing towards the 3,5-diphenyl isomer. These upfield peaks are found at $\delta 3.84 \text{ (dd, 1H)}$ and $\delta 3.40 \text{ (dd, 1H)}$; we observe two peaks because the product is diastereotopic with a stereocenter at carbon 5 and the adjacent H are in different chemical environments relative to the phenyl group on that carbon.

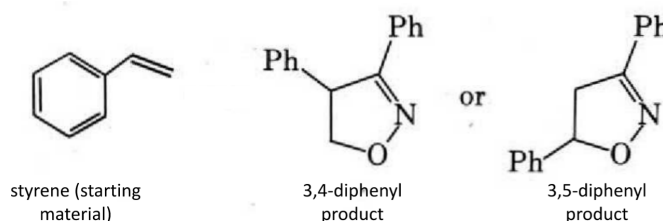


Figure 2: The possible 3,4-diphenyl and 3,5-diphenyl isomers (center and right structures, respectively) formed from the 1,3-dipolar cycloaddition with styrene (left structure) as the dipolarophile.

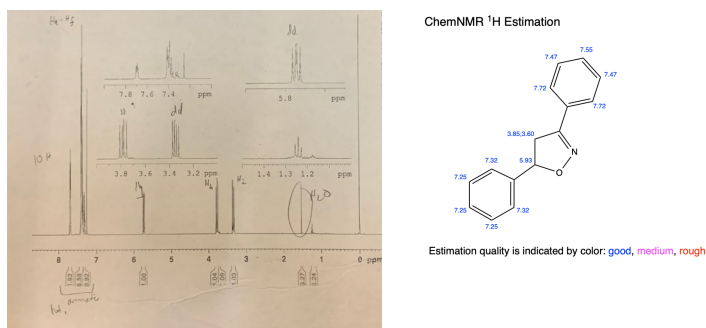


Figure 3: NMR spectrum (left) and ChemDraw depiction with predicted NMR chemical shifts (right) of our 3,5-diphenyl product from styrene cycloaddition. The predicted peaks generally match our spectrum.

A similar NMR spectral analysis of recrystallized product from our 4-chlorostyrene cycloaddition revealed that the 3,5-diphenyl isomer was exclusively formed (Figure 5). In this case, we report an NMR spectrum of crude product. The lack of recrystallization resulted in several starting material peaks in the spectrum. Nonetheless, our peaks match those predicted for the 3,5-diphenyl isomer, indicating it is likely exclusively favored here as well. Once again, we observe one relatively deshielded product H in the δ 5-6 ppm region (roughly, due to starting material presence), rather than two; and two product H in the δ 3-4 ppm region, matching the distribution of our 3,5-diphenyl product from styrene. It is possible that the steric hindrance of the phenyl rings prevents formation of the 3,4-diphenyl isomer, but more data would be required to confirm our hypothesis. Replacement of one or both phenyl groups followed by reaction and product structure analysis could inform us as to whether steric effects are a determining factor for this cycloaddition's regioselectivity.

We also found an electrostatic reason for the observed regioselectivity. Analysis in Spartan showed that the reacting C(H₂) of styrene is more negatively charged than the reacting C(H) (Table S1). The mechanism leading to the 3,5-diphenyl product matches this observation, since the more negative region of the dipolarophile would approach the positive carbon of the dipole, and the less negative region of the dipolarophile would be approached by the negative oxygen of the dipole (Figure 4).

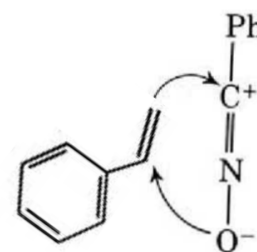


Figure 4: Reaction mechanism showing hypothetical proximity of styrene CH₂ to benzaldehyde oxime C and benzaldehyde oxime O to styrene CH.

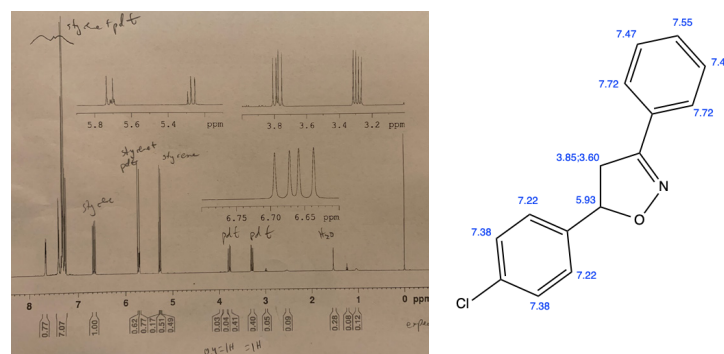


Figure 5: NMR spectrum (left) and ChemDraw depiction with predicted NMR chemical shifts (right) of our 3,5-diphenyl product from chlorostyrene cycloaddition. The predicted peaks can be found on our spectrum, as well as starting material peaks.

We also performed GC/MS analysis on our styrene addition product. The gas chromatograms included two significant peaks with retention times at 4.4 min and 13.2 min. The gas chromatogram and mass spectra were the same regardless of whether the reaction was performed in DCM or chloroform (Figure 6). Following analysis of their mass fragmentation patterns in the corresponding spectra, we identified these peaks as styrene and product, respectively (Figure 7). Our GC/MS data further support successful product formation that matches the 3,5-cycloaddition product. GC-MS analysis of our 4-chlorostyrene and acetoxystyrene bulk reactions confirmed that they formed the expected product, at least according to molecular weight (Figure 8). Collectively, these NMR, Spartan, and GC-MS findings confirm that the reaction proceeds according to the predictions in Gingrich and Pickering² and that the 3,5-diphenyl isomer is exclusively formed.

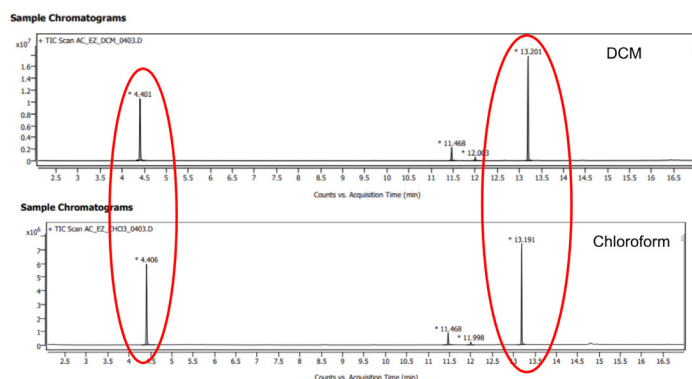


Figure 6: Chromatograms for crude product from styrene cycloaddition reactions in DCM and chloroform. As shown by the red circles, solvent choice between these two did not affect the formation of product. The small peaks at 11.5 min and 12.0 min are likely column debris, since the mass spectra contained large molecular ions that did not match the molecular weight of any of our reactants.

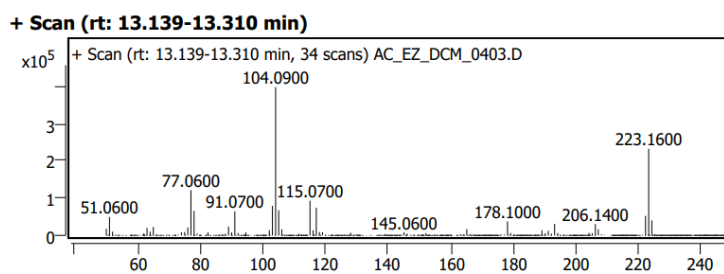


Figure 7: Mass spectrum of the product peak at 13.2 min. Our expected product molecular weight of 223 g/mol matches the m/z ratio of the mass ion in this spectrum, indicating that it corresponds to our styrene addition product.

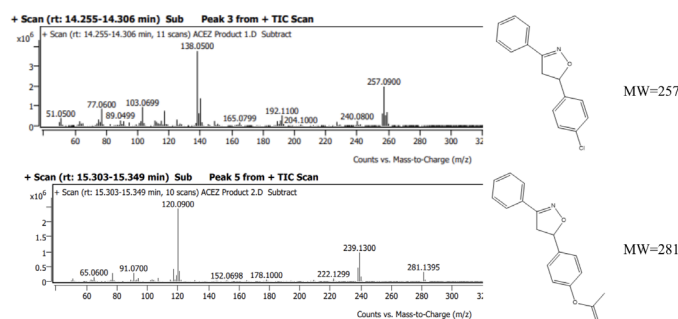


Figure 8: Mass spectra and structures with molecular weight of our 4-chlorostyrene and 4-acetoxystyrene products.

Kinetics and Rate Constants

Before settling on using NMR spectroscopy to acquire kinetics data, we attempted to measure reaction kinetics using UV/Vis spectroscopy as shown in Iwasaki et

al.³ and GC-MS. Although we could measure absorbance spectra for starting material and product, we were unable to detect a change in λ_{max} over time for our reaction, nor did we find a significant change in intensity at 265 nm (λ_{max} for our product) over time. We likely ran into this difficulty because styrene had a high absorbance at 250-260 nm that may have obscured an intensity change in the product peak. For future experiments, we would use the dipolarophile from Iwasaki et al.³ which absorbs in the visible range and ideally would allow us to accurately measure increasing product absorbance over time.

We also performed GC-MS on samples taken at regular time points from a bulk reaction with styrene as the dipolarophile and found that the relative integrations of product and anisole peaks did not appear to change over time (Figure 9). The fact that these peaks had reached a final integration value informed us that the reaction was likely occurring very quickly. It is also possible that the cycloaddition was continuing in the DCM solvent used for GC-MS; either way, the reaction ran effectively to completion before we could gather kinetic data using GC-MS.

In an attempt to more clearly measure the kinetics of the reaction, we repeated the styrene bulk reaction with some changes to sample collection. Performing a mini-extraction at each time point and immediately placing samples on ice gave strong trends for product formation as measured by GC relative to anisole and styrene peak integrations (Figure 10). Following this successful capture of changing relative amounts of product and starting material relative to anisole, we attempted an acetoxy bulk reaction with the same method of sample collection and an anisole reference peak. Unfortunately, our gas chromatogram was messy (Figure S2) and we were unable to find peaks with significant change in integration over time.

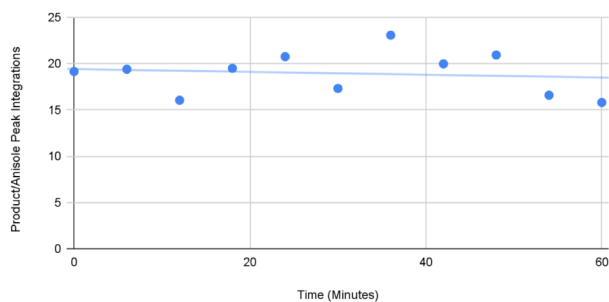


Figure 3- Ratio of Product to Anisole Peak Integrations vs. Time of Reaction.

Figure 9: Graph showing the ratio of product:anisole peak integrations versus time since reaction start. There is no relationship between time and product/anisole peak integration for this bulk reaction.

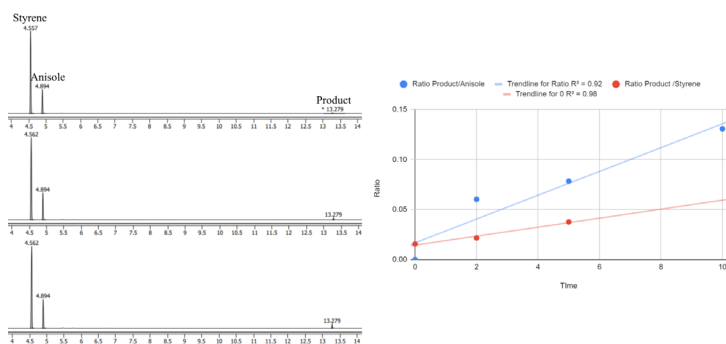


Figure 10- A) GC Chromatogram of reaction 2, 5, and 10 minutes after reaction start. B) GC peak integration product ratio trends when compared to anisole control and styrene starting material peaks.

Figure 10: Gas chromatograms for samples taken from the cycloaddition with styrene 2, 5, and 10 minutes after reaction start (left). Graph showing an increasing ratio of product:anisole and product:styrene peak integrations over time (right).

Following this finding, we further investigated NMR spectroscopy as a method for capturing kinetics data. Taking aliquots and making sure that the reaction was quenched would have been much more labor intensive than running the reaction in an NMR tube while collecting spectra over time. Running the reaction with active dipole in $CDCl_3$ allowed us to successfully take three spectra for a reaction with styrene showing changes in product peak integrations over time (Figure 11). Next, we collected NMR spectra of a run using acetoxystyrene over a full time frame from the combination of reactants to 30 minutes (Figure 12). These data also showed an increasing trend in product peak integrations over time, confirming that we could calculate rate constants using NMR spectra over time.

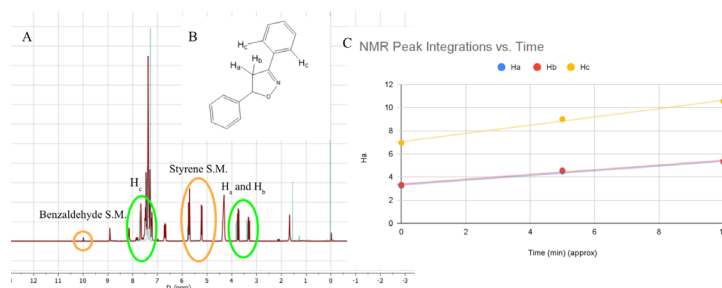


Figure 11- A) 1H NMR of purified product (light blue) and reaction mixture (red) with starting material and key product peaks marked. B) Product structure with key product peaks labeled. C) Trend of integrations of key product key peaks over kinetic test run.

Figure 11: A) Representative 1H NMR spectra of purified product (light blue background) and reaction mixture (red). B) Structure of product with significant H atoms labeled. C) Graph showing increasing trend of product peak integrations over time.

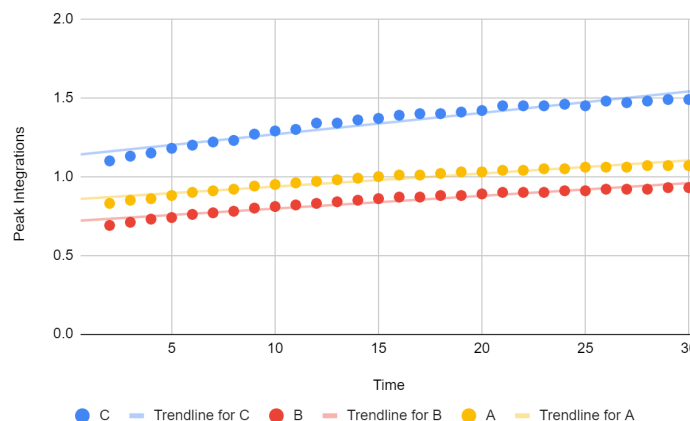


Figure 12: Graph showing increasing peak integrations for three different hydrogen atoms on the acetoxystyrene product. The hydrogen atoms of interest are equivalent to H_a (yellow), H_b (red), and H_c (blue) on the styrene product (Figure 11).

Comparing product peak integrations to the integration of the TMS peak with a known number of protons in the sample allowed us to calculate the changing concentration of product over time and calculate rate constants (Table 1). Our reactions are pseudo-first order since we included a large excess of dipolarophile (styrene or substituted styrene) into each reaction. We also calculated pseudo rate constants based on changing peak integrations rather than concentrations because the peak of interest overlapped starting material peaks in cyanostyrene.

We used our pseudo rate constants to produce

a Hammett plot (Figure 13). Using concentration-based rate constants produced a similar plot (Figure S5), so we used the pseudo rate constants to include our data point for cyanostyrene. Based on our ρ value of -0.194, it appears that electron-withdrawing group (EWG) substituents reduce the rate of the reaction and that electron-donating group (EDG) substituents increase the rate. This finding differs from our prediction that EWG substituents would increase the rate of the reaction based on styrene's role as the dipolarophile. One possible explanation for this observation is that, though EWG contributed favorably to the electrophilicity of the dipolarophile, they also deactivated the 2π electrons participating in the cycloaddition and therefore decreased the overall rate. By altering the method of dipole activation following Iwasaki et al.,³ scaling down the reaction, and running it in CDCl_3 (an alternative solvent to the original from Gingrich and Pickering²), we successfully captured rate data and used it to form trends with substituent σ values.

Dienophile	σ Value	k
Styrene	0	4.47×10^{-4}
Methylstyrene	-0.17	8.70×10^{-4}
Chlorostyrene	0.23	7.93×10^{-4}

Table 1: Rate constants (k) for the cycloaddition using various substituted styrenes. Rate constants are calculated using concentrations of product according to integration relative to the known quantity of TMS. See supporting information for an example graph and equation.

Dienophile	σ Value	k
Styrene	0	7.64×10^{-4}
Methylstyrene	-0.17	9.68×10^{-4}
Chlorostyrene	0.23	1.18×10^{-3}
Cyanostyrene	0.66	6.74×10^{-4}

Table 2: Pseudo rate constants for the cycloaddition using various substituted styrenes; these constants were calculated using $\ln[1/\text{product peak integration}]$ since the cyanostyrene product peak we have been using overlaps starting material

peaks and is therefore not a reliable measure of concentration. See supporting information for an example graph and equation.

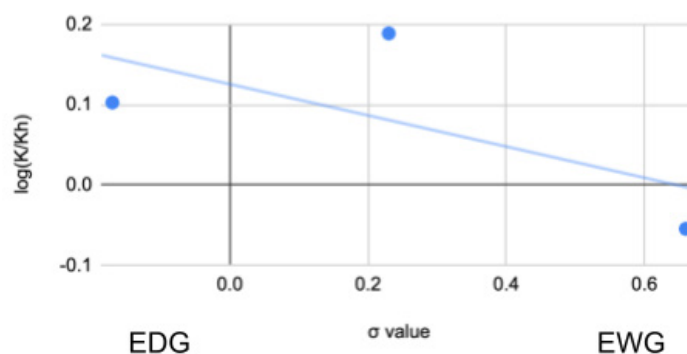


Figure 13: Hammett plot comparing σ value of substituents to $\log(K_r/K_h)$ using pseudo rate constant values for methylstyrene, chlorostyrene, and cyanostyrene. EWG substituents appear to reduce the reaction rate, $\rho = -0.194$ with $R^2 = 0.427$. K_r = rate for substituted reactant; K_h = rate for styrene.

HOMO/LUMO Gap Analysis and Comparison to Rate Data

To further explore the mechanism affecting rate, we analyzed Highest Occupied Molecular Orbital-Lowest Unoccupied Molecular Orbital (HOMO-LUMO) energy gaps in Spartan. Our *in silico* analysis indicated that more EWG substituents decrease the HOMO-LUMO energy gap between our dipole (activated benzaldehyde oxime) and dipolarophile (styrene or substituted styrene) (Figure 14). In contrast, EDG substituents appear to increase the gap. This trend makes sense since our 1,3-dipolar cycloaddition involves the HOMO of the dipole (benzaldehyde oxime) overlapping the LUMO of the dipolarophile (styrene or substituted styrene). EWG substituents on styrene generally lower the energy of the LUMO, decreasing the energy gap between its LUMO and the HOMO of our benzaldehyde oxime.

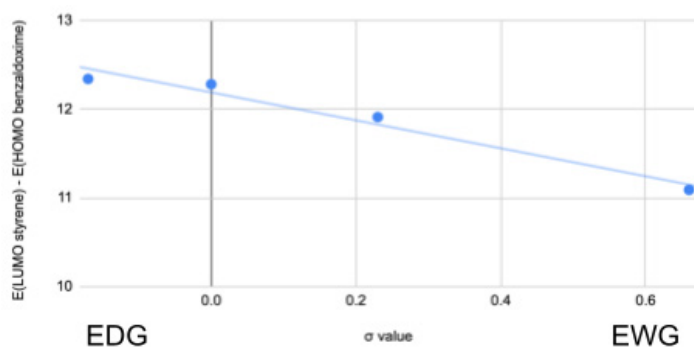


Figure 14: Hammett plot comparing σ value of substituents to the HOMO-LUMO energy gap between our starting benzaldehyde oxime and styrene or substituted styrene. EWG substituents appear to lower the energy gap, compared to EDG substituents which raise it.

These findings conflict with our Hammett plot for rate versus σ value (Figure 13). We expected that rate would increase as HOMO/LUMO gap decreased, but the rate appears to decrease according to our data points. It would be useful to replicate the point for cyanostyrene ($\sigma = 0.66$) since it is the one causing the regression to have a negative slope, which conflicts with the positive correlation we expected between rate and σ value. However, it is possible that this point is correct, since substituents on the dipolarophile of our reaction have been shown to increase then decrease rate in a V-shaped Hammett plot similar to ours.⁶ Following similar cycloaddition reactions, Holman et al.⁶ propose a radical pathway and changes in orbital interactions that might account for this difference in rate trend between EDG and EWG. We have documented an increasing-then-decreasing effect of substituent σ value on reaction rate; replication of our data would confirm this trend, which matches one found in the literature for a similar reaction.⁶

Activated Dipole Investigation

According to Iwasaki et al.,² the dipole stays activated in solution for at least 3h, and the authors used it within that time frame. We had leftover dipole in CDCl_3 from one week and used NMR spectroscopy to investigate whether the dipole remained activated over this longer time frame. We observed an absence of a significant peak at δ 8.2 ppm expected from inactive dipole starting material (Figure 15); this finding seemed to indicate that our dipole was still activated after one week. We compared the spectrum of the week-old dipole

to a spectrum of freshly prepared dipole (Figure 16) and saw even less of a peak at δ 8.2 ppm, though in both cases the peaks were relatively small. These findings contrasted with the NMR spectrum of our starting material benzaldehyde oxime (Figure S6) which did indeed have a significant peak at δ 8.2 ppm. Unfortunately, in contrast to our NMR findings, reactions with week-old dipole did not run, suggesting that other chemical changes are likely occurring that render the dipole unusable for our reaction.

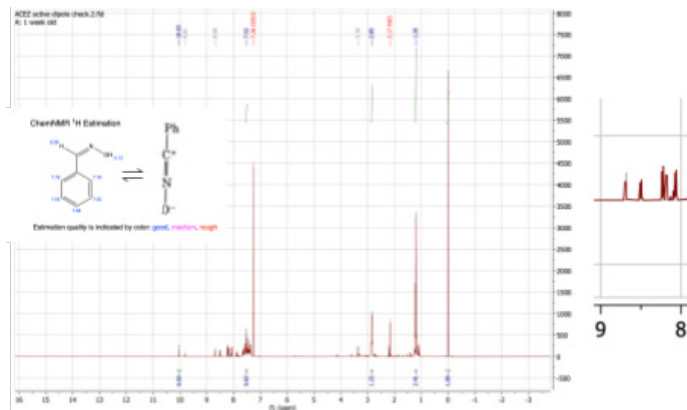


Figure 15: ChemDraw structure and predicted ^1H chemical shifts (left of equilibrium), structure of activated dipole from Gingrich and Pickering² (right of equilibrium), and ^1H NMR spectrum for activated dipole in CDCl_3 , one week after activation. There is a very minimal peak at δ 8.2 ppm, suggesting that the dipole is mainly in its active form, which lacks a peak there.

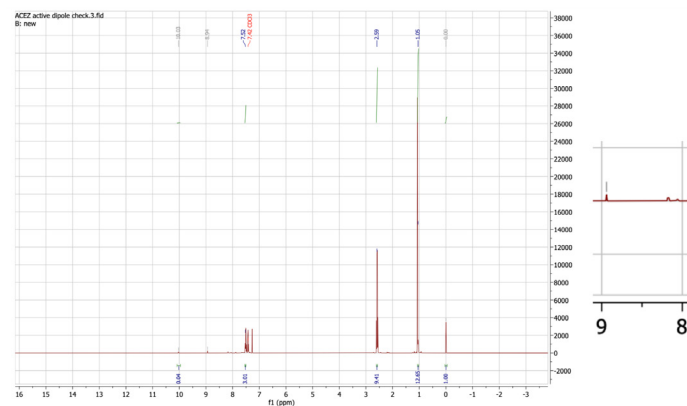


Figure 16: ^1H NMR spectrum for newly activated dipole in CDCl_3 . There is virtually no peak at δ 8.2 ppm, suggesting that the dipole is completely in its active form.

Conclusion

We originally set out to study the regioselectivity

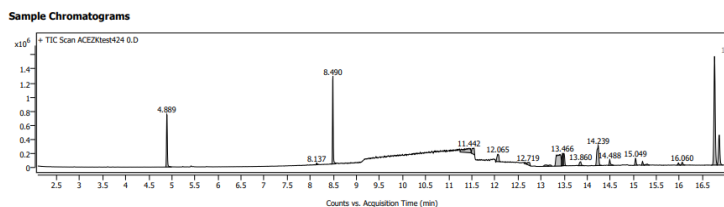


Figure S2: Representative gas chromatogram from a sample taken during our acetoxy bulk run. We were unable to find the peak changes necessary for acquiring kinetics data in these chromatograms.

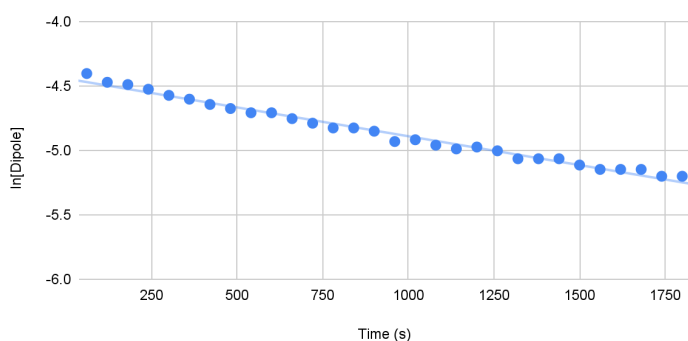


Figure S3: Rate plot for styrene; $k = -4.47 \times 10^{-4}$ M/s was calculated from $\ln[\text{styrene}]$ versus time.

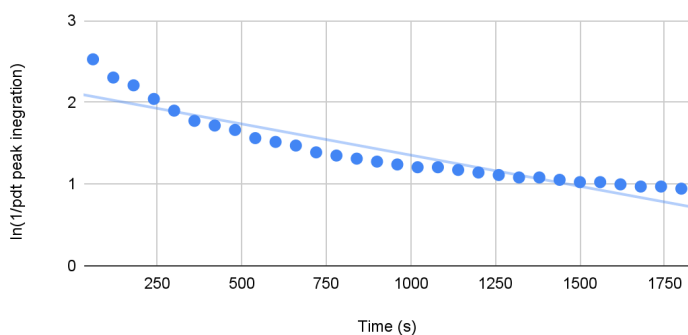


Figure S4: Pseudo rate constant plot for styrene; $k = -7.64 \times 10^{-4}$ M/s was calculated from $\ln[\text{styrene}]$ versus time.

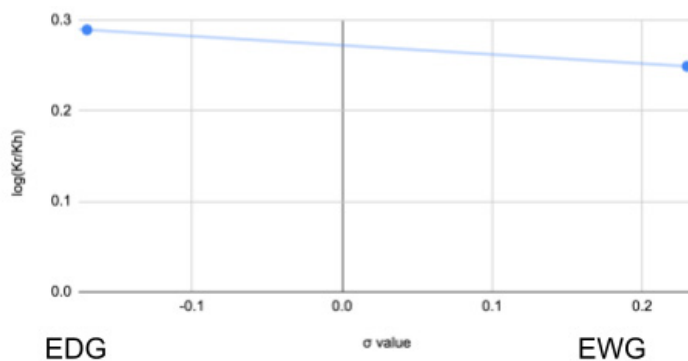


Figure S5: Hammett plot comparing σ value of substituents to $\log(K_r/K_h)$ using rate constant values for methylstyrene and chlorostyrene. EWG substituents appear to reduce the reaction rate, $\rho = -0.101$. K_r = rate for substituted reactant; K_h = rate for styrene.

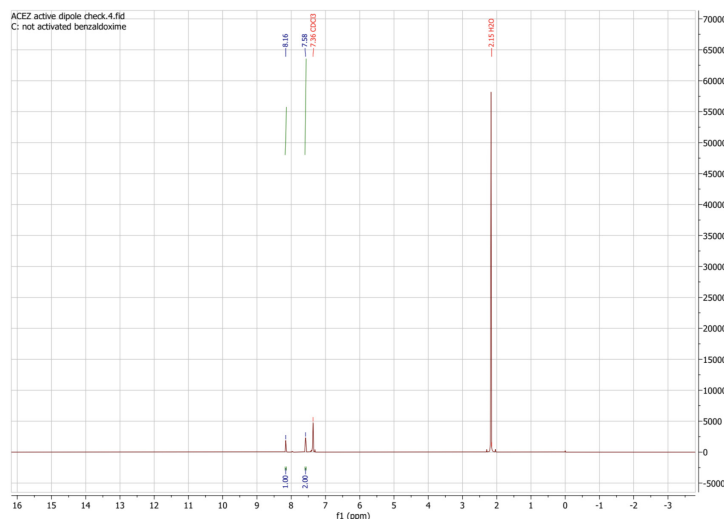


Figure S6: ^1H NMR spectrum of our benzaldehyde oxime starting material with a peak at δ 8.2 ppm integrating to 1H.